Chapter 5

Discussions

This chapter presents the discussion of the results obtained in chapter 4. The position and velocity distributions are present in section 5.1. Section 5.2 discuss the magnetic field. Finally suggestion for the future research are presented in section 5.3

5.1 Position and Velocity Distributions

From the results described in Chapter 4, the position distributions of the 1665-MHz OH maser features are shown in Figure 4.5. By comparing the positions and velocities of OH masers in this work and those of other masers, it is clear that infact the source, OH330.954-0.182 is the cluster a3 detected in this work. Figure 5.2 shows the positions of all masers after the (2.05 arcsec, -2.13 arcsec) offset in RA and Dec have been applied to those of Caswell (1995, 1998, 2001). The position of the OH masers at 6035 MHz is also agree well with cluster a7, which newly discovered in this observations. The position of 6.6-GHz methanol maser is therefore $\sim$ 8 arcsec southeastern of the 1.6 GHz OH maser cluster. Cluster a7 was not detected before this observations. If we focus on the northern clusters (a1 to a6), the position distribution surprisingly shows the ring shape. Figure 5.3 shows intensities and positions of 1665- and 1667-MHz maser features. The brightest features in both LHCP and RHCP are clustered in north-west region. At an assumed distance of $\sim$ 8.5 kpc (average value of Table 1 in Caswell (1998) the diameter (2a) of the ellipse is $\sim$ 1700 au.

Figure 5.4 shows the velocity distributions of OH masers along RA and declination axis. It can be seen that the masers have radial velocity gradient along RA axis. This is the evidence implying that the OH maser maybe associated with a rotating disk, with central radial velocity of the disk $\sim$ -90 km s^{-1}. Similar results have been found in recent studies of OH masers in massive star-forming regions associated with disks and outflows (W75N $\sim$ 10000 au (Hutawarakorn et al., 2002), AFGL 2591 $\sim$ 1500 au

(Hutawarakorn & Cohen, 2005) and ON1 $\sim$ 2000 au (Nammahachak et al., 2006)).

5.2 Magnetic Fields in OH330.953-0.182

From section 4.3, seven Zeeman pairs were detected in OH 330.953-0.182. Most of the Zeeman pairs were found in the western part of the ring with the mean value equal to -4.79 mG. If the Zeeman pair at the southern part of the region is taken into account, the mean magnetic field strength becomes -4.81 mG. The magnetic field strength of this level is sufficient for the field to be dynamically important in the star-forming regions. The magnetic fields play important roles in channeling the bipolar outflows observed in massive star-forming regions, e.g. in the case of G 35.2-0.74N (Hutawarakorn & Cohen, 1999), W75N (Hutawarakorn et al., 2002), NGC7538 (Hutawarakorn & Cohen, 2003), AFGL 2951 (Hutawarakorn & Cohen, 2005), (Hutawarakorn et al., 2002) and ON1 (Nammahachak et al., 2006).

In case of OH330.953-0.182, the magnetic field measured in the ring shape structure which could imply the magnetic field in the disk. However, currently there are no evidence of the molecular outflow in this source.

5.3 Suggestion for Future Research

It is useful to study multi-transitions of masers. Position and velocity distribution of masers found to be associated, e.g. in case of OH 1.6 GHz and excited OH masers at 6 GHz. Therefore, it maybe interesting to observe excited OH maser at 6 GHz in more details, i.e. higher resolution, in order to study the region.

The position and velocity distributions of OH masers studied in the work suggest a rotating disk structure. It will be useful to observe other molecular lines to gain more evidences supporting disk and outflow structures commonly found in massive star-forming regions.The typical molecular lines which should be observed are NH_3 and CS as traces for large scale disk structure, and CO as a trace for the outflow.

Moreover, the velocity and position of OH masers could be tested in the disk

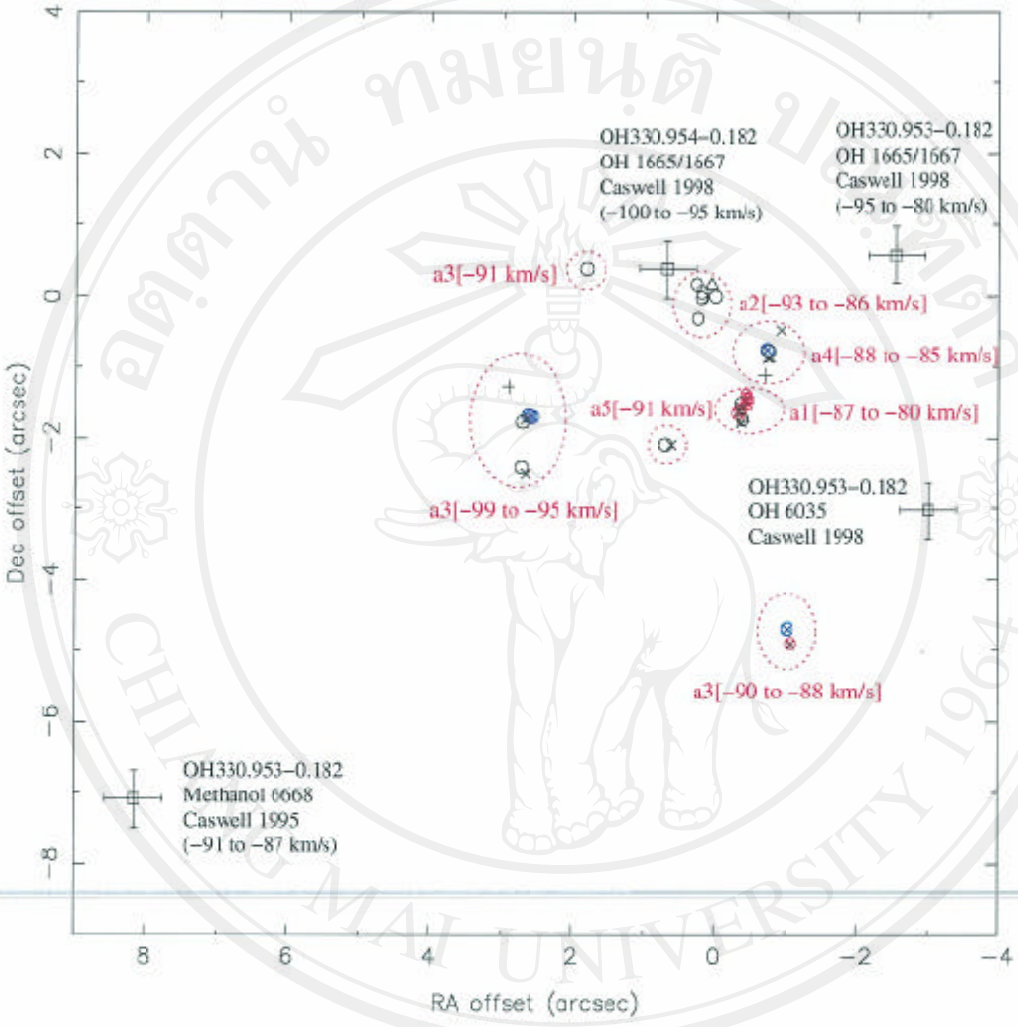

Figure 5.1: Position distribution of OH 330.953-0.182. Symbols are denoted the frequency and the polarization (plus signs for LHCP 1667-MHz, triangles for RHCP 1667-MHz, crosses for LHCP 1665-MHz and circles for RHCP 1665-MHz in this study. Square with the position errors include positions of OH masers and other maser previous observed in the literature.

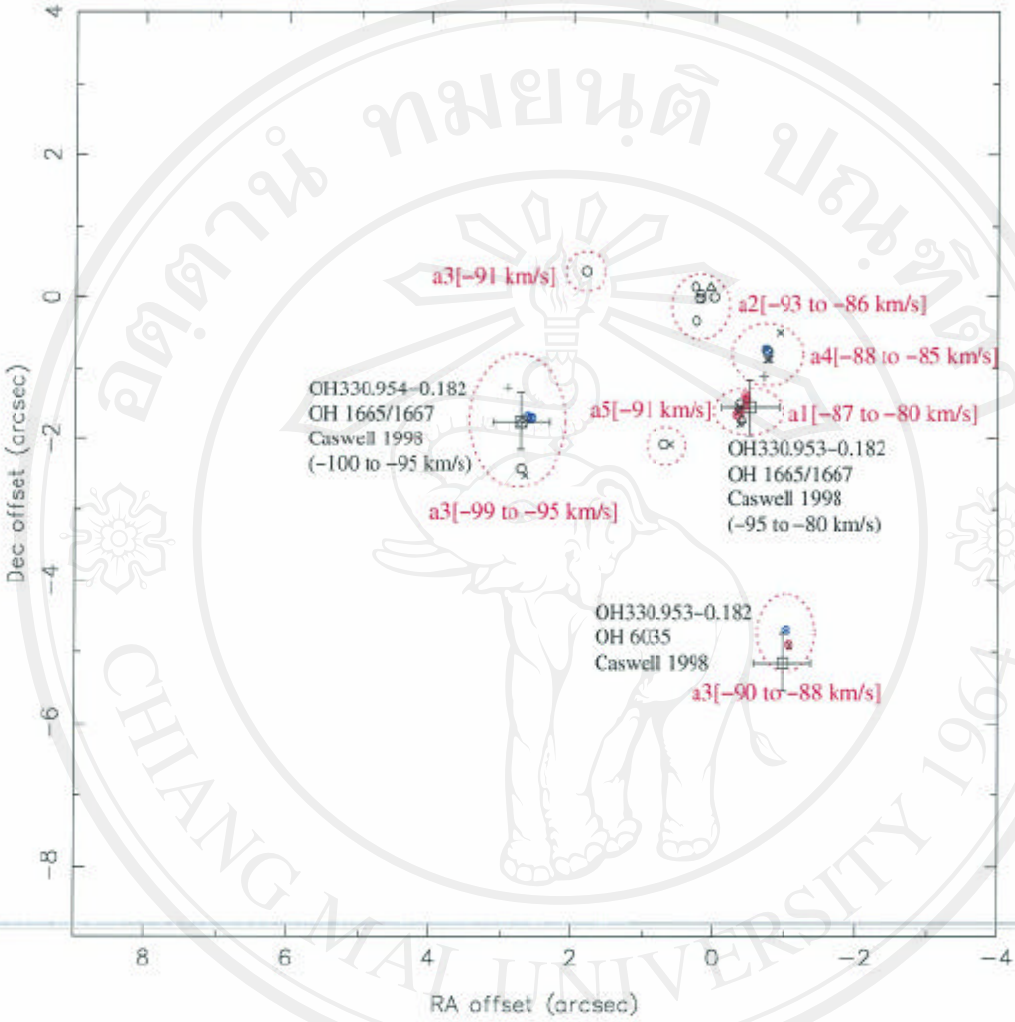

Figure 5.2: Position distribution of OH 330.953-0.182 maser features after shift (2.05 arcsec, -2.13 arcsec) offset. Symbols are denoted the frequency and the polarization (plus signs for LHCP 1667-MHz, triangles for RHCP 1667-MHz, crosses for LHCP 1665-MHz and circles for RHCP 1665-MHz in this study. Square with the position errors include positions of OH masers and other maser previous observed in the literature.

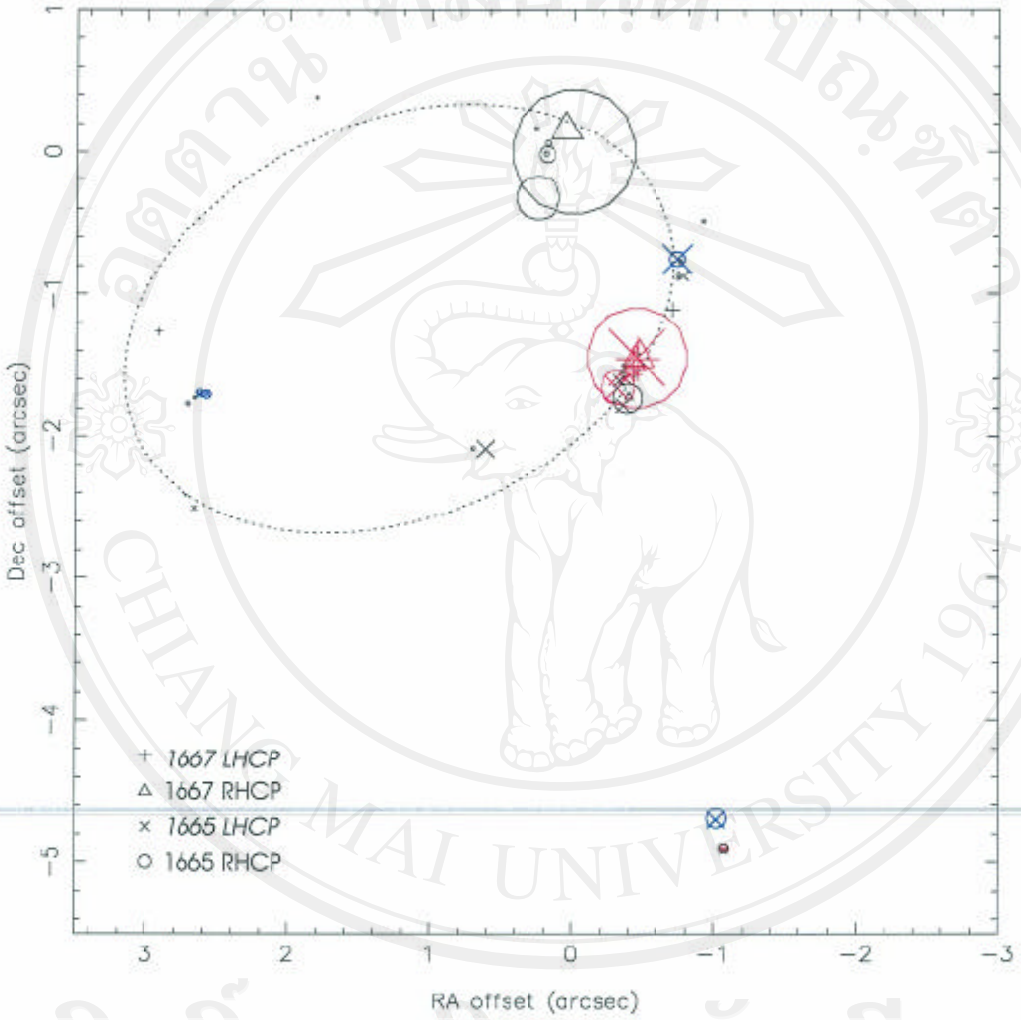

Figure 5.3: Intensity distribution of the 1665- and 1667-MHz OH maser features. The size of each symbol is proportional to the peak flux density.

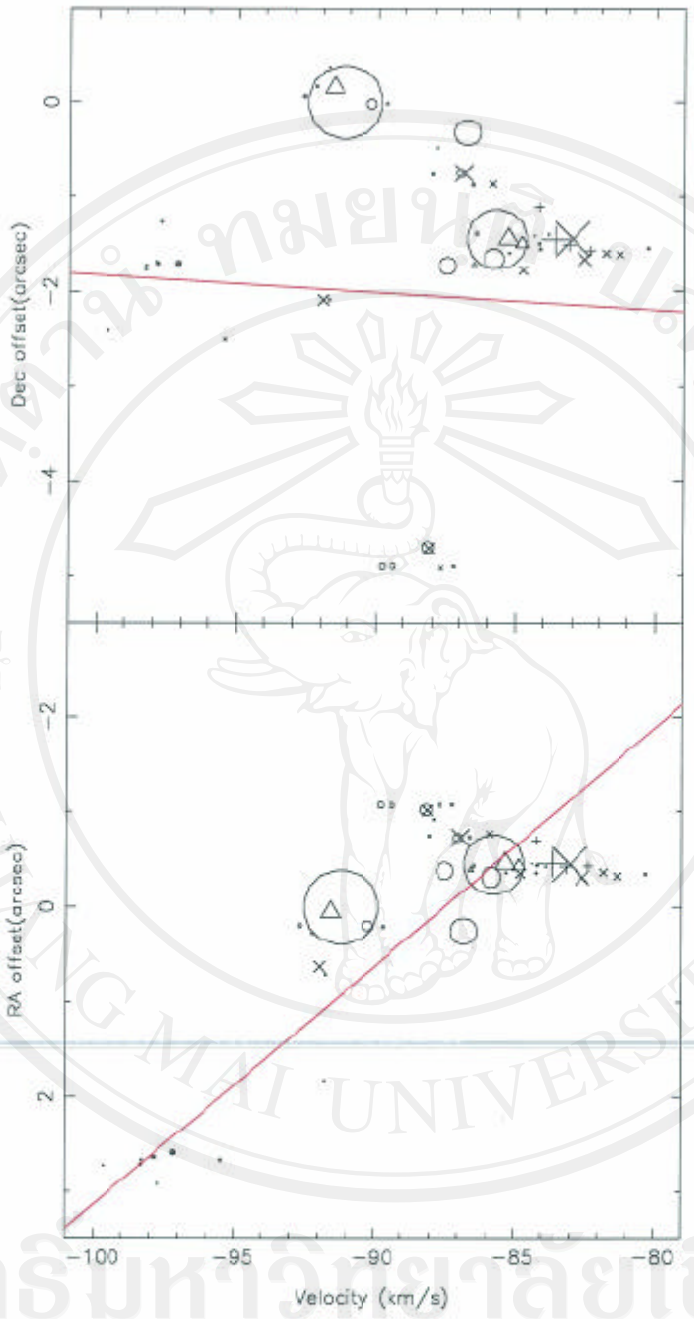

Figure 5.4: Plot of radial velocity against RA and declination, for the 1665- and 1667-MHz OH masers in OH330.953-0.182. Symbols are denoted the frequency and the polarization (plus signs for LHCP 1667-MHz, triangles for RHCP 1667-MHz, crosses for LHCP 1665-MHz and circles for RHCP 1665-MHz). The size of each symbol is proportional to the peak flux density.

and outflow modeling programme by Cohen et al. (2006) for further confirmation to this work.

Finally, the full polarisation observations of the 1.6 GHz OH masers and excited OH masers at 6 GHz will be crucial for more detailed study of the magnetic field configurations in this region.